1521-009X/49/7/563–571$35.00
DRUG METABOLISM AND DISPOSITION
https://doi.org/10.1124/dmd.121.000359
Drug Metab Dispos 49:563–571, July 2021

Hepatic Scaling Factors for In Vitro–In Vivo Extrapolation of Metabolic Drug Clearance in Patients with Colorectal Cancer with Liver Metastasis[S]

Areti-Maria Vasilogianni, Brahim Achour, Daniel Scotcher, Sheila Annie Peters, Zubida M. Al-Majdoub, Jill Barber, and Amin Rostami-Hodjegan

Centre for Applied Pharmacokinetic Research, Division of Pharmacy and Optometry, School of Health Sciences, University of Manchester, Manchester, United Kingdom (A.-M.V., B.A., D.S., Z.M.A.-M., J.B., A.R.-H.); Translational Quantitative Pharmacology, BioPharma, R&D Global Early Development, Merck KGaA, Darmstadt, Germany (S.A.P.); and Certara, Inc. (Simcyp Division), Sheffield, United Kingdom (A.R.-H.)

Received January 5, 2021; accepted April 5, 2021

ABSTRACT

In vitro–in vivo extrapolation (IVIVE) linked with physiologically based pharmacokinetics (PBPK) modeling is used to predict the fates of drugs in patients. Ideally, the IVIVE-PBPK models should incorporate systems information accounting for characteristics of the specific target population. There is a paucity of such scaling factors in cancer, particularly microsomal protein per gram of liver (MPPGL) and cytosolic protein per gram of liver (CPPGL). In this study, cancerous and histologically normal liver tissue from 16 patients with colorectal liver metastasis were fractionated to microsomes and cytosol. Protein content was measured in homogenates, microsomes, and cytosol. The loss of microsomal protein during fractionation was accounted for using corrections based on NADPH cytochrome P450 reductase activity in different matrices. MPPGL was significantly lower in cancerous tissue (24.8 ± 9.8 mg/g) than histologically normal tissue (39.0 ± 13.8 mg/g). CPPGL in cancerous tissue was 42.1 ± 12.9 mg/g compared with 56.2 ± 16.9 mg/g in normal tissue. No correlations between demographics (sex, age, and body mass index) and MPPGL or CPPGL were apparent in the data. The generated scaling factors together with assumptions regarding the relative volumes of cancerous versus noncancerous tissue were used to simulate plasma exposure of drugs with different extraction ratios. The PBPK simulations revealed a substantial difference in drug exposure (area under the curve), up to 3.3-fold, when using typical scaling factors (healthy population) instead of disease-related parameters in cancer population. These indicate the importance of using population-specific scalars in IVIVE-PBPK for different disease states.

SIGNIFICANCE STATEMENT

Accuracy in predicting the fate of drugs from in vitro data using IVIVE-PBPK depends on using correct scaling factors. The values for two of such scalars, namely microsomal and cytosolic protein per gram of liver, is not known in patients with cancer. This study presents, for the first time, scaling factors from cancerous and matched histologically normal livers. PBPK simulations of various metabolically cleared drugs demonstrate the necessity of population-specific scaling for model-informed precision dosing in oncology.

Introduction

Cancer is a multifaceted disease characterized by deregulated cell growth with the potential to invade tissues and form metastases. Colorectal cancer is the third most common type of cancer and is associated with the second highest number of deaths caused by cancer (Bray et al., 2018). Metastasis to the liver constitutes one of the main causes of mortality in patients with colorectal cancer (Siegel et al., 2018), as it accounts for 70% of metastases from colorectal cancer, followed by metastasis to the lungs, distant lymph nodes, and peritoneum (Holch et al., 2017). Metastasis to the liver can affect hepatic function, as the resultant lesions occupy space in liver tissue leading to abnormal liver function tests (Jiang et al., 2018). Inflammation is a condition that may also affect the hepatic function, as inflammatory markers have been shown to be associated positively with the size of metastases (Wong et al., 2007).

Challenges in the development of new drugs in the area of oncology include the difficulty of recruiting from the appropriate patient population and safety issues when testing anticancer drugs of high toxicity in healthy volunteers (Gutierrez et al., 2009; Bates et al., 2015). Given these challenges, and the high medical need, model-informed precision

This work was supported by Merck KGaA, Frankfurter St. 250, F130/005, 64293 Darmstadt, Germany.

A.R.-H. holds shares in Certara, a company focusing on Model-Informed Drug Development, and declares no support from any organization for the submitted work. All other authors declare that they have no conflicts of interest.

https://doi.org/10.1124/dmd.121.000359.

[S] This article has supplemental material available at dmd.aspetjournals.org.

ABBREVIATIONS: ALC, all liver cancerous; ALN, all liver normal; AUC_{0-inf}, area under the curve from time 0 to infinity; BMI, body mass index; Cancer-D, cancer-default population; CPPGL, cytosolic protein per gram of liver; CRLM, colorectal liver metastasis; HomPPGL, homogenate protein per gram of liver; IVIVE, in vitro–in vivo extrapolation; MFT, Manchester University National Health Service Foundation Trust; MPPGL, microsomal protein per gram of liver; P450, cytochrome P450; PBPK, physiologically based pharmacokinetics; PK, pharmacokinetics; T_{max}, time at which C_{max} is observed.

dosing and, in particularly, physiologically based pharmacokinetics (PBPK) are widely employed (Darwich et al., 2017). PBPK modeling has generally higher regulatory acceptance in the development of anticancer drugs than other disease areas (Yoshida et al., 2017), and models are used to inform dosing of patients with cancer.

In vitro–in vivo extrapolation (IVIVE) employs models that incorporate systems information and in vitro drug data to predict plasma and tissue concentration-time profiles, which are critical components of bottom-up PBPK models (Rostami-Hodjegan, 2012). Data obtained using population-specific in vitro systems taking into account potential differences in functional activity need to be scaled to in vivo outcomes. For IVIVE of hepatic drug clearance, different in vitro systems can be used, including recombinantly expressed enzymes, hepatocytes, liver microsomes, and cytosol. The scalars related to liver microsomes and cytosol are microsomal protein per gram of liver (MPPGL) and cytosolic protein per gram of liver (CPPGL), respectively (Barter et al., 2007).

To obtain microsomal and cytosolic fractions required for in vitro data, it is necessary to homogenize liver tissue and fractionate the homogenate using differential centrifugation. During tissue fractionation, membrane protein is subject to significant losses (Wilson et al., 2003). Accounting for protein losses is necessary for obtaining correct MPPGL values and, thus, more accurate clearance predictions. For the correction of microsomal protein loss, different microsomal markers can be used, such as NADPH cytochrome P450 reductase or total P450 content measured in the homogenate and microsomal fractions (Barter et al., 2008). Cytosolic markers for the correction of cytosolic protein loss include alcohol dehydrogenase and glutathione-*S*-transferase (Cubitt et al., 2011); however, loss of cytosolic protein is expected to be negligible (soluble fraction). MPPGL and CPPGL values have been reported in healthy human liver with mean values of 32 mg/g liver and 80.7 mg/g liver, respectively (Barter et al., 2007; Cubitt et al., 2011).

Although scalars have been reported for healthy liver, such data are scarce in disease populations, such as cancer. Available scalar data in liver cancer suggest that MPPGL is different in livers with hepatocellular carcinoma relative to normal liver tissue (Zhang et al., 2015; Gao et al., 2016). To our knowledge, there are no reports of scalars or IVIVE-PBPK models for colorectal liver metastasis (CRLM) for the prediction of in vivo hepatic drug clearance. The aim of this study was to generate MPPGL and CPPGL scaling factors in cancerous liver tissue from patients with CRLM and compare the values with scalars from matched histologically normal tissue. The scalars were applied in PBPK simulations to predict in vivo hepatic clearance. This study highlights the importance of applying appropriate population-specific scalars for IVIVE of metabolic drug clearance in patients with CRLM.

Materials and Methods

Materials and Chemicals. All chemicals were purchased from Sigma-Aldrich (Poole, Dorset, UK) unless otherwise stated. EDTA-free protease inhibitor cocktail was obtained from Roche Applied Sciences (Mannheim, Germany).

Liver Samples. Matched cancerous and histologically normal liver tissue specimens from 16 adult patients with CRLM were obtained opportunistically after hepatectomy from the Manchester University National Health Service Foundation Trust (MFT) Biobank, Manchester, UK. The study was covered under the MFT Biobank generic ethics approval (NRES 14/NW/1260 and 19/NW/0644). Among the 16 donors, seven were female and nine were male, and their ages ranged from 34 to 85 years. The body mass index (BMI) of the patients ranged from 21.6 to 36.3 kg/m^2. Supplemental Table 1 presents demographic and clinical details of the donors.

Preparation of Human Liver Microsomal and Cytosolic Fractions. Microsomal and cytosolic fractions were generated from liver tissue using differential centrifugation as previously described (Achour et al., 2017). Liver tissue was homogenized by a mechanical homogenizer (Thermo Fisher Scientific, UK) in homogenization buffer (150 mM KCl, 2 mM EDTA, 50 mM Tris, 1 mM dithiothreitol, and EDTA-free protease inhibitor cocktail, pH 7.4) at 10 ml for each gram of liver tissue. The homogenate was centrifuged at 10,000 *g* for 20 minutes at 4°C using an Optima L-100 ultracentrifuge (Beckman Coulter, Fullerton, CA). The first pellet (cell debris) was stored at −80°C, and then the supernatant was further centrifuged at 100,000 *g* for 75 minutes at 4°C. The cytosol (the supernatant) was stored at −80°C, and the pellet (microsomes) was resuspended in 1 ml of storage buffer (0.25 M potassium phosphate, pH 7.25) per gram of liver tissue and stored at −80°C.

Measurement of Total Protein Content in Homogenates and Fractions. The protein content of liver homogenates, microsomes, and cytosolic samples was measured using bicinchoninic acid protein assay (Pierce Microplate BCA protein assay Kit – Reducing Agent Compatible) in triplicate. Absorbance was measured at 562 nm using a SpectraMax 190 platereader (Molecular Devices, Sunnyvale, CA) with bovine serum albumin used as calibration standard. For the homogenates and the cytosolic samples that contained dithiothreitol, a compatibility reagent solution was used. The CPPGL and the homogenate protein per gram of liver (HomPPGL) were calculated based on the total protein content, and no further correction for loss was required.

Measurement of NADPH Cytochrome P450 Reductase Activity. In the current study, NADPH P450 reductase activity was used to account for microsomal membrane loss during fractionation. The activity of NADPH P450 reductase was measured in homogenates and microsomes from the same liver samples to estimate loss of microsomal protein during fractionation. The protocol was adapted from methods by Guengerich et al. (2009) and Achour et al. (2011). In a 1-ml cuvette, oxidized equine cytochrome c (0.5 mM, 80 µL) was mixed with potassium phosphate buffer (0.25 M, 980 µl, pH 7.25), KCN (1 mM, 10 µl), and homogenates (10 µl, equivalent to 1 mg of tissue) or 1:10 diluted microsomes (10 µl, equivalent to 1 mg of tissue). The absorbance of the mixtures was measured using a Jenway 7315 UV-visible spectrophotometer (Thermo Fisher Scientific) at 550 nm in kinetic mode. The absorbance was monitored for 2 minutes to establish the baseline, followed by addition of reduced NADPH solution (10 mM, 10 µl) to start the reaction of cytochrome c reduction, which was monitored for 5 minutes.

The slope of the initial linear phase of the reaction is directly proportional to the amount of cytochrome P450 reductase in the sample. The enzyme activity (units/mg liver tissue) was calculated using eq. 1, and fractional loss of microsomal protein was estimated based on the ratio of activity in microsomes relative to the homogenate from the same liver sample (eq. 2) using the ratio of the slope from the microsomal fraction (1 mg of tissue) to the slope from the homogenate (1 mg of total protein) for each individual. The ratios also allowed calculation of microsomal membrane enrichment. MPPGL for each sample was corrected using the recovery factors according to eq. 3 (Barter et al., 2008). Recovery factor is equal to 1-fractional loss of microsomal protein.

$$Enzyme\ activity = \frac{\triangle A_{550}/min \times dil \times total\ volume}{21.1 \times V} \quad (1)$$

where ΔA550/min represents the rate of change in the absorbance at 550 nm, dil represents the dilution factor of the original enzyme sample, total volume is the volume of the reaction mixture (ml), 21.1 is the extinction coefficient for reduced cytochrome c (mM^{-1} cm^{-1}), and V represents the volume of the enzyme sample (ml) corresponding to 1 mg of liver tissue.

$$Microsomal\ loss = 1 - \frac{activity\ in\ microsomes}{activity\ in\ homogenate} \quad (2)$$

$$MPPGL\ \left(mg\ g^{-1}\right) = \frac{Yield\ of\ microsomal\ protein\ \left(mg\ g^{-1}\right)}{1 - Fraction\ loss\ of\ microsomal\ protein} \quad (3)$$

Statistical Data Analysis. Statistical data analysis was performed, and graphs were generated using GraphPad Prism 8.1.2 (La Jolla, CA). The data are presented as mean ± S.D. CV was used to describe variability in datasets, and the Kolmogorov-Smirnov test was used to assess the normality of distribution of the datasets. Several datasets did not follow normal distribution, and therefore nonparametric statistical tests for differences were used. Differences in HomPPGL, uncorrected MPPGL, and CPPGL values between histologically normal and matched cancerous tissues were assessed using Wilcoxon test. Differences in MPPGL values between histologically normal and matched cancerous tissues were assessed using Mann-Whitney test. This test was also used for the assessment of the effect of hepatic lobe of origin and sex of donors on MPPGL and CPPGL in normal and cancerous tissues. For the assessment of the effect of BMI and age on MPPGL and CPPGL, Spearman correlation and linear regression analysis were used. In each of the above cases, the probability cut-off value for statistical significance was set at 0.05.

Physiologically Based Pharmacokinetic Simulations. The effect of using the generated scaling factors in a cancer population was assessed using PBPK modeling on Simcyp V18 Release 1 (Certara, Sheffield, UK) in healthy and cancer populations. For the assessment of effects of MPPGL changes on simulated plasma drug exposure, four cytochrome P450 substrates with different hepatic extraction ratios (see Table 1) were used: alfentanil (predominantly metabolized by CYP3A4), alprazolam (predominantly metabolized by CYP3A4 and CYP3A5), midazolam (predominantly metabolized by CYP3A4 and CYP3A5), and desipramine (predominantly metabolized by CYP2D6). P450 isoforms are responsible for the metabolism of the majority of clinically used drugs in all fields of treatment (anticancer and non–anti-cancer drugs), with CYP3A4/5 being the most prevalent, followed by CYP2D6. For this reason, we used CYP3A4, CYP3A5, and CYP2D6 enzymes for our simulations.

The compound files were not changed from those provided within the Simcyp simulator. PBPK simulations were performed using system parameters already available on the simulator for healthy ("Sim-Healthy Volunteers") and cancer ("Sim-Cancer") virtual populations, without or with inclusion of MPPGL data measured in current study. The effects of MPPGL changes in cancer on drug exposure after oral administration were assessed using four different MPPGL models:

MPPGL model 1 (Healthy; healthy population): the default MPPGL in Simcyp was used for the healthy population; mean MPPGL was 39.8 mg/g tissue (defined by the Simcyp model), (eq. 4, Barter et al., 2008).

$$Mean\ MPPGL\ \left(\frac{mg}{g}\right) = 10\text{^}(1.407 + 0.0158\ *\ Age - 0.00038\ *\ Age\ \text{^}2\ +\ 0.000024\ *\ Age\ \text{^}3) \quad (4)$$

For eq. 4, the CV% is 26.9.

MPPGL model 2 (Cancer-D; cancer-default population): the default MPPGL in Simcyp was used for the cancer population; mean MPPGL was 39.8 mg/g tissue (defined by the Simcyp model), (eq. 4, Barter et al., 2008).

These two models were used to assess any effects on drug exposure between healthy and cancer populations without changing MPPGL values. The key differences in the systems parameters between Healthy and Cancer-D involve age distribution, hematocrit, α1-acid glycoprotein, and albumin levels.

MPPGL model 3 (New Cancer-ALN; new cancer population-assuming liver is obtained from patients with cancer, but entire liver tissue is histologically normal, therefore ALN is defined as "all liver normal"): experimentally derived MPPGL in histologically normal tissue was used for the cancer population; mean MPPGL was 39 mg/g tissue, (eq. 5, adapted from Barter et al., 2008 with revised baseline).

$$Mean\ MPPGL\ \left(\frac{mg}{g}\right) = 10\text{^}(1.59106462) \quad (5)$$

For eq. 5, CV% is 35.36.

Model 3 assumes that the whole liver remains histologically normal, and this implies the maximum metabolic capacity of microsomal enzymes. CV% used for this model is experimentally derived based on MPPGL in histologically normal tissue.

MPPGL model 4 (New Cancer-ALC; new cancer population-assuming liver is obtained from patients with cancer, and entire liver tissue is histologically cancerous, therefore ALC is defined as "all liver cancerous"): experimentally derived MPPGL in cancerous tissue was used for the cancer population; mean MPPGL was 24.8 mg/g tissue, (eq. 6, adapted from Barter et al., 2008 with revised baseline).

$$Mean\ MPPGL\ \left(\frac{mg}{g}\right) = 10\text{^}(1.3944516) \quad (6)$$

For eq. 6, CV% is 39.7.

Model 4 assumes that the whole liver is cancerous, and this implies the minimum metabolic capacity of microsomal enzymes. It also assumes that the liver mass does not change, and that each pmol of enzyme has the same activity, irrespective of disease state. CV% used for this model is experimentally derived based on MPPGL in cancerous tissue.

The size of the liver being normal is important, as this will define how much of the liver will be fully functional. If a proportion of liver is not normal, this may lead to decreased scaled intrinsic clearance, with effect on clearance being compound dependent. In cases of a surgical resection, clearance should be calculated based on healthy MPPGL and remnant liver size. Although surgical resection is the ideal solution for patients with CRLM, this is not feasible for many patients that have to live with a liver with histologically normal and cancerous parts, with unchangeable liver size. Therefore, metabolic capacities of enzymes come from two different sources: histologically normal and cancerous liver (relative contributions of normal and cancerous parts are unknown in the current study). In this case, it is more appropriate to use MPPGL for histologically normal tissue with the weight of the liver being histologically normal and MPPGL for cancerous tissue with the weight of the liver being cancerous.

For eq. 4, the age was plotted against MPPGL values for Healthy population; for both observed and predicted (Barter et al., 2008) values (Supplemental Fig. 1). For each model and for each drug, a generic trial design was used, with the following characteristics. The age range of the cancerous donors is 34–85 and the age range in the virtual population is 20–50 years old, which consists a limitation of our study. However, this limitation wouldn't have any effect on the final observations, as the age range is kept consistent in all the models, and additionally, age-dependent MPPGL in cancer samples was not apparent (Fig. 4D). The mean (for all 100 virtual subjects) systemic concentration-time profiles were plotted, and the area under the curve from time 0 to infinity ($AUC_{0\text{-}inf}$) and C_{max} values were compared across the four MPPGL methods/models (Table 1). Parameters used for PBPK simulations are listed in Supplemental Table 2. Oral doses for alfentanil, alprazolam, midazolam, and desipramine are 0.043 mg/kg, 0.5 mg, 5 mg, and 50 mg, respectively.

Lack of differences in CPPGL between normal and cancerous tissue (see *Results*) meant that significant effects on the clearance and systemic concentrations of drugs metabolized by cytosolic enzymes were not expected. Therefore, no PBPK simulations were performed to assess possible effects on pharmacokinetics of drugs metabolized by cytosolic enzymes.

Results

Protein Content of Liver Homogenates and Fractions. Total protein content was measured in homogenates, microsomes, and cytosols from histologically normal and matched cancerous ($n = 16$) liver samples (Fig. 1; Supplemental Table 3). The mean HomPPGL was 126.1 ± 46.7 mg/g in histologically normal samples and 86.9 ± 50.2 mg/g in matched cancer samples (range: 75.1–266.7 and 37.1–204.8 mg/g, respectively). The mean CPPGL was 56.2 ± 16.9 mg/g in histologically normal samples and 42.1 ± 12.9 mg/g in cancer samples (range: 32.3–80.7 and 24.8–67.2 mg/g, respectively). There was no statistically significant difference in HomPPGL (Wilcoxon test, $P = 0.0654$) and CPPGL between histologically normal and cancerous samples

TABLE 1

Mean predicted E_H, T_{max}, C_{max}, and $AUC_{0\text{-}inf}$ for oral alfentanil, alprazolam, midazolam, and desipramine using four different scaling methods within PBPK model. $AUC_{0\text{-}inf}$ ratios using different methods are also provided

For each simulation, 10 trials and 10 subjects per trial were included. Healthy: default MPPGL (Simcyp) with a healthy population. Cancer-D: default MPPGL with a cancer population. New Cancer-ALN: MPPGL measured in this study for histologically normal tissue with a cancer population. New Cancer-ALC: MPPGL measured in this study for cancer tissue with a cancer population.

Drug	Model	E_H	C_{max}	$AUC_{0\text{-}inf}$	T_{max}	Relative $AUC_{0\text{-}inf}$ Ratios to Healthy
			ng/ml	*ng/ml.h*	*h*	
Alfentanil	Healthy	0.36	24	59	0.6	
	Cancer-D	0.24	33	120	0.9	2
	New Cancer-ALN	0.25	33	120	0.9	2
	New Cancer-ALC	0.17	39	193	0.9	3.3
Alprazolam	Healthy	0.04	8	144	1.2	
	Cancer-D	0.04	8	142	1.2	1
	New Cancer-ALN	0.04	8	140	1.2	1
	New Cancer-ALC	0.03	8	199	1.3	1.4
Midazolam	Healthy	0.43	24	76	0.6	
	Cancer-D	0.48	21	65	0.6	0.9
	New Cancer-ALN	0.48	21	65	0.5	0.9
	New Cancer-ALC	0.38	27	104	0.6	1.4
Desipramine	Healthy	0.42	16	1385	5.9	
	Cancer-D	0.34	17	1421	5.9	1
	New Cancer-ALN	0.35	17	1406	5.9	1
	New Cancer-ALC	0.27	19	1989	6.4	1.4

E_H, hepatic extraction ratio.

(Wilcoxon test, $P = 0.0654$). The mean microsomal protein isolated from liver, before correction for membrane loss, was 15.8 ± 3.9 mg/g in histologically normal samples and 6.5 ± 3.3 mg/g in matched cancer samples (8.8–22.8 and 2.6–15.2 mg/g, respectively), and a 2.4-fold statistically significant difference (Wilcoxon test, $P < 0.0001$).

NADPH Cytochrome P450 Reductase Activity in Homogenates and Microsomes. Activity of NADPH cytochrome P450 reductase was used to assess recovery and enrichment of microsomal membrane. Activity measurements were made in homogenates and microsomal fractions of histologically normal ($n = 16$) and matched cancer samples ($n = 11$) (Fig. 2A and Supplemental Table 4). Activity measurements in five tumorous samples were below the limit of quantitation and thus, only data for 11 tumorous samples are presented. The mean enzymatic activity in homogenates was 2.36 ± 0.73 units/mg in histologically normal tissues, and 0.58 ± 0.37 units/mg of tissue in cancer samples (range: 0.8–3.58 and 0.14–1.42 units/mg, respectively). In microsomal fractions, activity was 1.03 ± 0.44 units/mg of tissue in histologically normal tissues and 0.18 ± 0.19 units/mg of tissue in cancer samples (range: 0.34–1.72 and 0.03–0.71 units/mg of tissue, respectively).

Enrichment and recovery of microsomal proteins relative to homogenates were calculated for histologically normal ($n = 16$) and matched cancerous samples ($n = 11$), as shown in Fig. 2, B and C, respectively. Mean enrichment was 3.5- ± 1.5-fold (range: 1.5–7.3) for histologically normal and 3.3 ± 1.4 (range: 1.4- to 5.7-fold) for cancerous samples. Microsomal protein recovery was 0.4 ± 0.2 (range: 0.2–0.8) for histologically normal and 0.3 ± 0.1 (range: 0.1–0.5) with minimal difference in mean recovery for the normal (0.4) and cancerous samples (0.3).

Corrected Microsomal Protein per Gram of Liver. The MPPGL values were corrected using the recovery factors for histologically normal ($n = 16$) and cancer tissues ($n = 11$) (Fig. 3). The mean corrected MPPGL was 39 ± 13.8 mg/g histologically normal tissue and 24.8 ± 9.8 mg/g cancerous tissue (range: 16.5–63.1 mg/g and 8.7–43.9 mg/g, respectively). MPPGL values were significantly lower in tumorous samples compared with histologically normal samples (Mann-Whitney test, $P = 0.0109$).

Effect of Demographics on MPPGL Values. The effects of anatomic origin of liver tissue (left or right liver lobe), sex, BMI, and age on MPPGL values were tested for histologically normal and cancerous tissues (Fig. 4). Some demographics information is not available for each sample. For example, the liver lobe (right or left) from which the sample has been taken is not available for three of the patients. Similarly, BMI is not available for three of the patients. Therefore, only 13 samples are used for the correlation of liver lobe or BMI with MPPGL. The mean MPPGL was 38.7 ± 13.1 mg/g in histologically normal tissue from the left liver lobe ($n = 4$; 25.4–56.1 mg/g) and 37.0 ± 14.4 mg/g in histologically normal tissue from the right liver lobe ($n = 9$; 16.5–61.0 mg/g). By contrast, MPPGL was 29.4 ± 4.3 mg/g in cancerous tissue from the left liver lobe ($n = 2$; 26.3–32.4) and 22.4 ± 7.7 mg/g in cancerous tissue from the right liver lobe ($n = 7$; 8.7–32.7 mg/g). The difference in MPPGL from different lobes for histologically normal was not statistically significant (Mann-Whitney test, $P = 0.9399$). The statistical test was not applied to data from tumorous samples due to the low sample size from the left liver lobe ($n = 2$) (Fig. 4A). The MPPGL was 38.3 ± 14.3 mg/g and 39.5 ± 14.3 mg/g for female ($n = 7$; 6.5–56.1 mg/g) and male ($n = 9$; 25.4–63.1 mg/g) donors of histologically normal tissue, respectively. MPPGL was 23.3 ± 7.2 mg/g and 26.0 ± 12.2 mg/g for female ($n = 5$; 12.9–32.7 mg/g) and male ($n = 6$; 8.7–43.9 mg/g) donors of cancerous tissues, respectively. No significant differences in MPPGL between male and female donors of histologically normal (Mann-Whitney test, $P = 0.8371$) and tumorous tissues were observed (Mann-Whitney test, $P > 0.9999$) (Fig. 4B). There was no trend in MPPGL values with BMI (Spearman test, $P = 0.6338$) or age (Spearman test, $P = 0.8711$) (Fig. 4, C and D, respectively).

Effect of Demographics on CPPGL Values. The effects of anatomic origin of tissue (left or right liver lobe), sex, BMI, and age on CPPGL values were tested for histologically normal and cancerous tissues (Fig. 5). Some demographics information is not available for each sample. For example, the liver lobe (right or left) from which the sample has been taken is not available for three of the patients. Similarly, BMI is not available for three of the patients. Therefore, only 13 samples are used for the correlation of liver lobe or BMI with CPPGL. The mean CPPGL was 47.7 ± 11.1 mg/g in histologically normal tissue from the left liver lobe ($n = 4$; 33.9–57.7 mg/g) and 58.3 ± 18.8 mg/g in histologically normal tissue from the right lobe ($n = 9$; 32.3–80.7 mg/g). CPPGL was 45.2 ± 11.4 mg/g in cancerous tissue from the left liver lobe ($n = 4$; 30.8–54.6 mg/g) and 38.5 ± 11.5 mg/g in cancerous tissue from the right liver lobe ($n = 9$; 24.8–58.6 mg/g). There was no statistically significant difference in CPPGL from different lobes for histologically normal (Mann-Whitney test, $P = 0.3301$) or tumorous samples (Mann-Whitney test, $P = 0.6042$) (Fig. 5A). The CPPGL was 61.4 ± 14.9 mg/g and 52.2 ± 18 mg/g for female ($n = 7$; 34.1–77.1 mg/g) and male ($n = 9$; 32.3–80.7 mg/g) donors of histologically normal tissue, respectively. CPPGL was 37.8 ± 12.4 mg/g and 45.5 ± 12.9 mg/g for female ($n = 7$; 24.8–54.8 mg/g) and male ($n = 9$; 30.8–67.2 mg/g) donors of cancerous tissues. There was no statistically significant difference in CPPGL between male and female donors of histologically normal (Mann-Whitney test, $P = 0.2991$) or tumorous tissues (Mann-Whitney test, $P = 0.1738$) (Fig. 5B). There was no specific

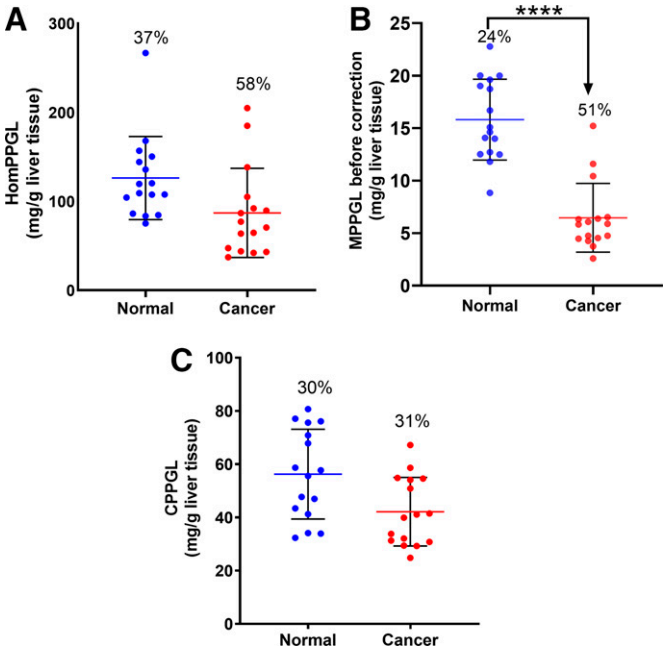

Fig. 1. Total protein content (mg per gram of liver) in homogenates [HomPPGL (A)], microsomal fractions [MPPGL before correction for losses (B)] and cytosolic fractions [CPPGL (C)] from histologically normal and matched tumor samples ($n = 16$). The MPPGL values in (B) are not corrected for loss of membrane protein. Blue and red symbols represent normal and cancer samples. The lines represent means, error bars represent S.D.s, and percentages represent CV. The asterisks (****) represent statistical differences with $P < 0.0001$ between histologically normal and cancerous tissues. Wilcoxon test was used for comparison of HomPPGL, uncorrected MPPGL, and CPPGL between matched cancerous and histologically normal samples.

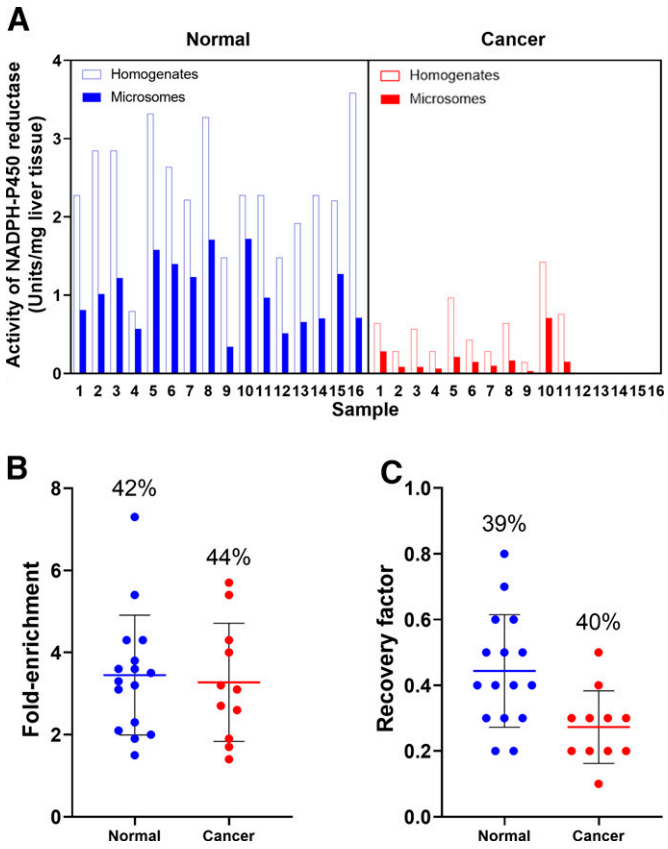

Fig. 2. Activity of NADPH cytochrome P450 reductase in homogenates and microsomes from histologically normal (n = 16) and tumor samples (n = 11) from patients with CRLM (A). Each bar represents the mean value of triplicate measurements of each individual sample. Blue open and solid bars correspond to normal homogenates and microsomes, respectively. Red open and solid bars correspond to cancer homogenates and microsomes, respectively. Fold-enrichment (B) and recovery (C) of microsomal proteins from histologically normal (n = 16) and tumor (n = 13) samples from patients with CRLM. Lines represent means, error bars represent S.D.s, and percentages represent CV. Blue and red symbols represent histologically normal and tumor samples, respectively.

correlation between CPPGL values and BMI (Spearman test, P = 0.2191) or age (Spearman test, P = 0.27415) (Fig. 5, C and D, respectively).

Physiologically Based Pharmacokinetic Simulations. Simulations for four different drugs (alfentanil, alprazolam, midazolam, and desipramine) were performed using four different methods (Fig. 6); model 1 (Healthy) used default MPPGL (Simcyp) with a healthy population, model 2 (Cancer-D) used default MPPGL with a cancer population, model 3 (New Cancer-ALN) used MPPGL measured in this study in histologically normal tissue with a cancer population, and model 4 (New Cancer-ALC) used MPPGL measured in this study in cancer tissue with a cancer population. Table 1 lists pharmacokinetic parameter values (T_{max}, C_{max}, and $AUC_{0\text{-}inf}$) for all simulations. C_{max} is the maximum drug concentration observed in plasma, and T_{max} is the time at which the highest drug concentration occurs after drug administration. $AUC_{0\text{-}inf}$ is the area under the plasma drug concentration-time curve from time 0 to infinity. New Cancer-ALN assumes that the whole liver is histologically normal, whereas New Cancer-ALC assumes that the whole liver is cancerous. For alfentanil, $AUC_{0\text{-}inf}$ predicted using MPPGL of cancerous tissue (New Cancer-ALC) was approximately 3.3-fold higher of that obtained using default MPPGL (Simcyp) with a healthy population (Healthy), whereas for midazolam, alprazolam, and desipramine, this value was approximately 1.4-fold higher.

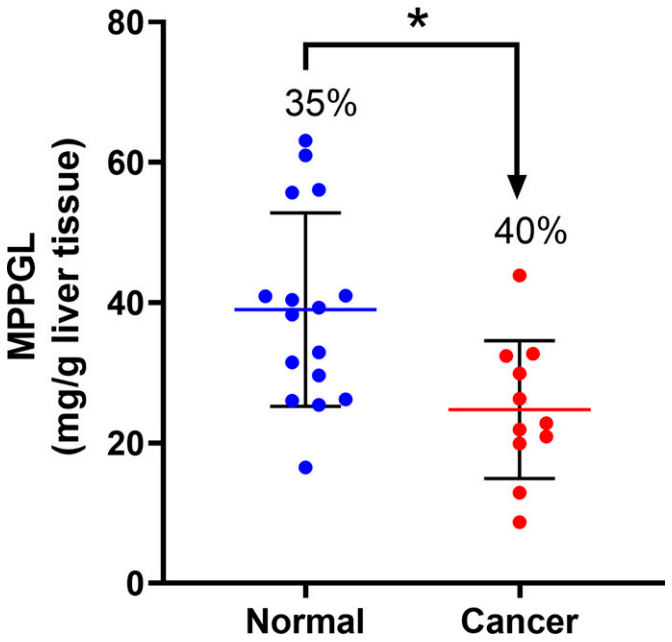

Fig. 3. Corrected microsomal protein content (mg) per gram tissue (MPPGL) from histologically normal (n = 16) and tumor samples (n = 11). Lines represent means, error bars represent S.D.s, and percentages represent CV. The asterisk (*) represents statistical difference (Mann-Whitney test, $P < 0.05$).

Discussion

Scaling factors, including MPPGL and CPPGL, are used for IVIVE of data generated in in vitro systems to predict metabolic clearance of drugs (Wilson et al., 2003; Barter et al., 2007; Cubitt et al., 2011). Interindividual variability of MPPGL has been reported previously (Wilson et al., 2003; Barter et al., 2008) and may explain part of the variation in metabolic clearance in the absence of genetic differences in the abundance and activity of enzymes in individuals. The data describing scalars in special populations and in disease states, such as cancer, are scarce. In addition, the effects of changes in these scalars (MPPGL, CPPGL) in patients with cancer on metabolic clearance have not been investigated. As cancer is not a uniform disease (for example, drug metabolizing enzymes and transporters may vary in different cancer types), the effects in each cancer type should be addressed independently. Changes in MPPGL for primary hepatocellular carcinoma compared with histologically normal tissue have been reported (Zhang et al., 2015; Gao et al., 2016), but corresponding data for metastatic liver cancer are currently lacking. To our knowledge, our study is the first to describe scaling factors for CRLM.

In this study, CPPGL and HomPPGL values were measured as the total protein content of each fraction, whereas MPPGL was calculated by correcting for protein loss during fractionation using cytochrome P450 reductase activity, a microsomal membrane marker. MPPGL values for histologically normal tissues (39.0 ± 13.8 mg/g of tissue) were consistent with the literature (Pelkonen et al., 1973; Wilson et al., 2003; Barter et al., 2007; Zhang et al., 2015), whereas values in cancerous tissues were significantly lower (24.8 ± 12.9 mg/g of tissue). A difference in the CV% was also observed between the histologically normal (CV% = 35) and the cancer tissues (CV% = 40). Higher CV% in cancer tissues may reflect the heterogeneity of cancer tissues or the different number of samples (smaller in cancer) that could increase the variability in cancer. The global reduction in microsomal protein content suggests that the abundance (pmol/g liver) of microsomal proteins, such as cytochrome P450 enzymes, in liver tissue may

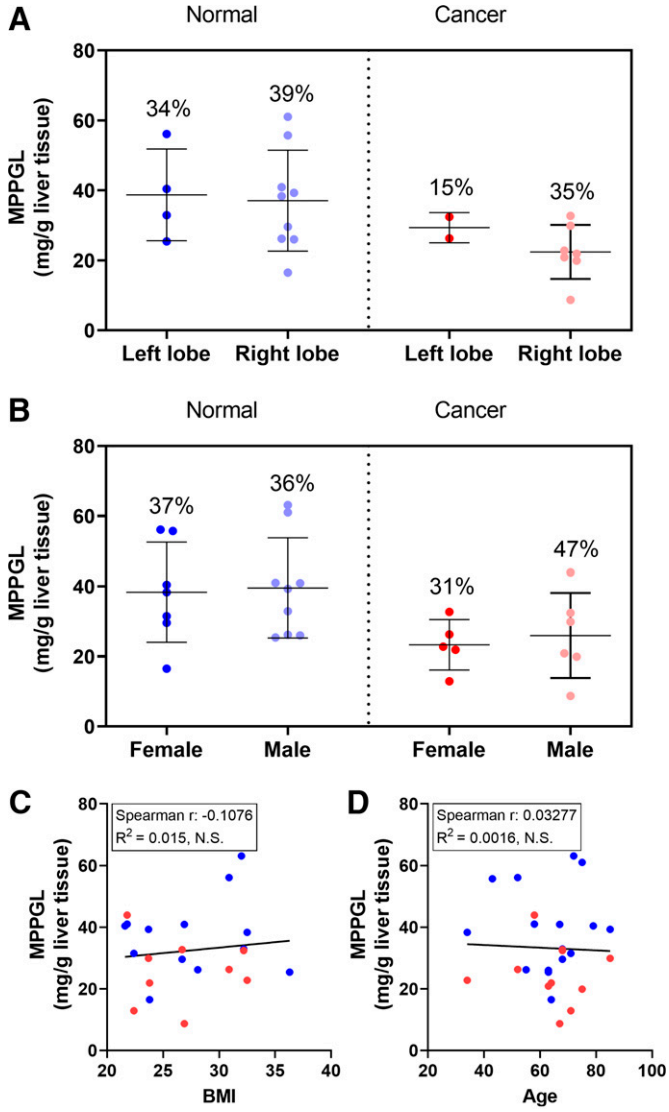

Fig. 4. Effects of liver lobe (A), sex (B), BMI (C), and age (D) on MPPGL values for histologically normal and cancer samples. In (A) and (B), lines represent means, error bars represent S.D. values, and percentages represent CV. Mann-Whitney test was used to assess the effect of hepatic lobes and sex. Spearman correlation and linear regression were used to assess the effect of BMI and age. Blue symbols represent histologically normal samples, and red symbols represent cancer samples. N.S. means no significant relation ($P > 0.05$).

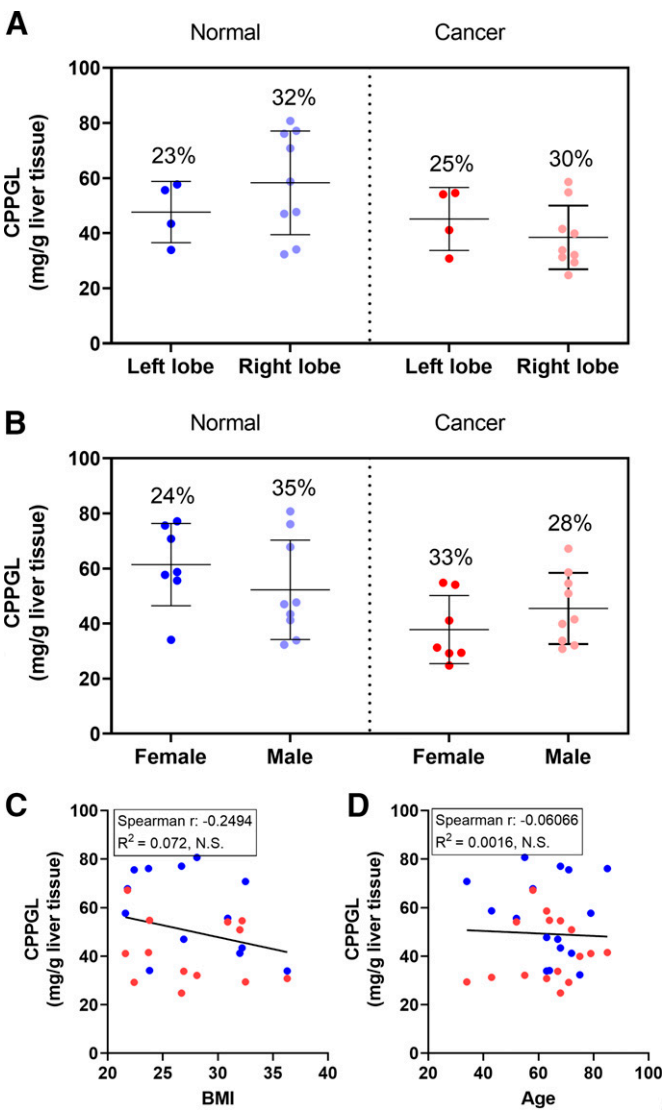

Fig. 5. Effects of liver lobe (A), sex (B), BMI (C) and age (D) on CPPGL values for histologically normal and cancer samples. In (A) and (B), lines represent means, error bars represent S.D. values, and percentages represent CV. Mann-Whitney test was used to assess the effect of hepatic lobes and sex. Spearman correlation and linear regression were used to assess the effect of BMI and age. Blue symbols represent histologically normal samples and red symbols represent cancer samples. N.S. means no significant relation ($P > 0.05$).

decrease in CRLM. Reported data on cytochrome P450 are limited to qualitative evidence that identify specific enzymes in histologically normal and tumorous tissues from patients with CRLM (Lane et al., 2004), and therefore, future proteomics studies involving quantification of such enzymes would be valuable. Functional activity studies with probe substrates would also be useful but require larger samples than are available to us currently. CPPGL and HomPPGL values showed little difference between cancerous and histologically normal tissues, and CPPGL in histologically normal tissue (56.2 ± 16.9 mg/g of tissue) was consistent with the literature (45–134 mg/g) (Boogaard et al., 1996; Renwick et al., 2002; Mutch et al., 2007).

The potential effects of donor demographics (such as age, sex, BMI) and sampled liver lobe on MPPGL and CPPGL values were evaluated. Statistical analysis showed no relationship between the examined variables and changes in MPPGL and CPPGL values. Barter et al. (2007) performed a meta-analysis of literature data from 114 individuals and reported a relationship between age and MPPGL; values decreased with increasing age (40 mg/g liver for a 30-year-old individual and 31 mg/g liver for a 60-year-old individual). This effect of age on MPPGL had not been discernible in the component individual studies (Pelkonen et al., 1974; Lipscomb et al., 1998, 2003; Wilson et al., 2003; Hakooz et al., 2006). A more recent study by Barter et al. (2008) showed that MPPGL values increased from childhood until the age of 28 years, then decreased thereafter. The small sample size and large underlying variability in the data of the present study meant that any correlation of MPPGL with age could not be delineated. Likewise, BMI did not affect MPPGL and CPPGL in either normal or cancerous tissues based on data from this study. There is no published literature on correlation between BMI and MPPGL or CPPGL in cancer. The sex of donors had no discernible effect on MPPGL or CPPGL in normal or cancerous tissues, consistent with earlier studies (Schmucker et al., 1990; Wilson et al., 2003). In addition, the liver lobe from which the tissues were

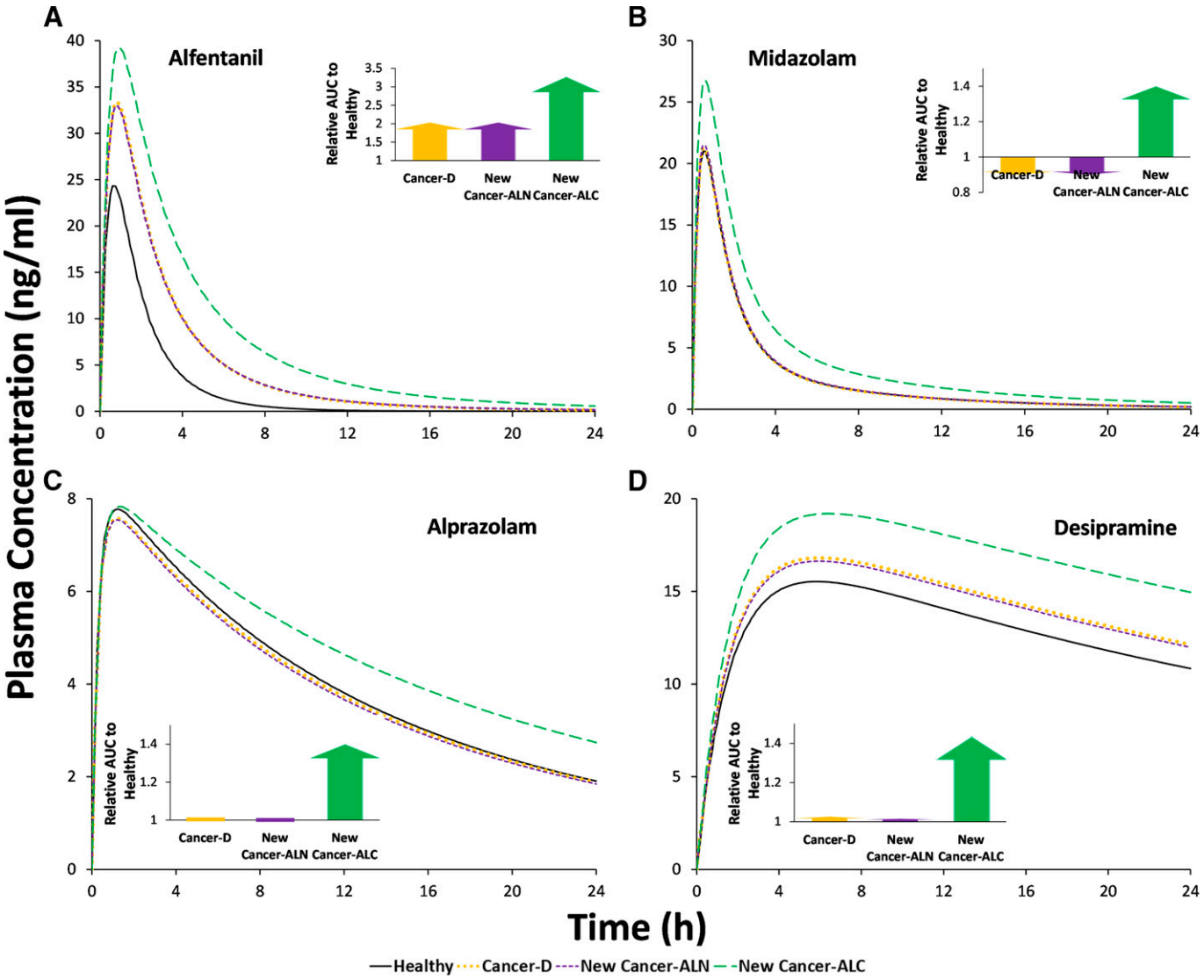

Fig. 6. Mean predicted systemic concentration over time (24 hours) after oral administration of alfentanil (A), midazolam (B), alprazolam (C), and desipramine (D). For each drug, four different methods of scaling were used. Healthy: default MPPGL (Simcyp) with a healthy population. Cancer-D: default MPPGL with a cancer population. New Cancer-ALN: MPPGL measured in this study for histologically normal tissue with a cancer population. New Cancer-ALC: MPPGL measured in this study for cancer tissue with a cancer population. Inset graphs show the Relative $AUC_{0\text{-inf}}$ ratios of Cancer-D, New Cancer-ALN, and New Cancer-ALC to Healthy.

sampled did not have an effect on MPPGL or CPPGL values from either normal or cancerous tissues. There are no reported data in the literature about regional differences in human liver, but studies in mice showed that microsomal P450 activity is variable in different lobes (Rudeck et al., 2018). Additionally, there was an effort to correlate the MPPGL values to the disease severity. No trend was observed, although the way that the samples were categorized according to the disease severity was not completely quantitative. This is a result of the small number of samples, and the lack of the information about the disease severity for all the patients.

The impact of applying different MPPGL values as scalars was studied using PBPK simulations on different drugs (alfentanil, alprazolam, midazolam, desipramine) metabolized by P450 enzymes with different extraction ratios. Generally, PK profiles of drugs are expected to differ in cancer populations compared with profiles in healthy subjects. In many cases, clearance of anticancer drugs decreases in patients with cancer compared with healthy individuals (Piotrovsky et al., 1998; Houk et al., 2009; Hudachek et al., 2010) for various reasons, including comorbidities, such as hepatic and renal impairment in patients with cancer (Suri et al., 2015). Another possible reason may be changes in MPPGL or CPPGL and differences in the expression of enzymes and transporters (Gao et al., 2016; Billington et al., 2018). Our data showed little difference in CPPGL between normal and cancerous tissues, but significantly lower MPPGL in cancer samples. Therefore, only the effect of MPPGL on drug pharmacokinetics was assessed in the simulations. MPPGL was used in other studies for scaling in hepatocellular carcinoma and glioblastoma (Gao et al., 2016; Li et al., 2017), and the present study is the first to assess the effect of changes in MPPGL in CRLM. The results for all the drugs showed that the MPPGL value affected drug exposure, suggesting that the proportion of the liver affected by cancer affects drug levels reaching the systemic circulation. More specifically, when the whole liver was assumed to

be tumorous, higher systemic concentration was predicted compared with a histologically normal liver. Our simulations show that using appropriate MPPGL values for a certain population is important for the prediction of drug exposure; however, the applied MPPGL value should be accompanied by the percentage of cancerous liver in each patient. Although the percentage of cancerous liver is not known for the present study, it is common practice for major hepatectomy to resect up to 70% of the total liver for a sufficient liver function, including histologically normal and cancerous tissue (Hemming et al., 2003; Jiang et al., 2018). As a result, there may be a significant contribution of the tumor to the overall liver activity in patients with CRLM. If we know the proportion of normal to cancerous tissue for an individual, then such data can be incorporated into the PBPK model. Otherwise, sensitivity and uncertainty analysis should be performed between two extreme cases (100% normal versus 100% cancerous) to establish worst-case scenario. It is important to clarify that the predicted PK profiles are not compared with clinical data, which are not available for patients with CRLM. Therefore, our simulations are not indicative of which method is correct with observations, but they point out the assumption that MPPGL affect the PK in patients with cancer. Further work is needed to verify this updated PBPK cancer population model against clinical data. PK may also depend on cancer stage, starting with a small amount of liver being affected (New Cancer-ALN) resulting in a high amount of liver being cancerous (New Cancer-ALC). In this study, we assumed that the abundance of P450s in CRLM was the same as for the generic healthy and cancer population in Simcyp. Although there are no published data on the abundance in CRLM, potential differences in the abundance of P450s may have additive effects on the PK (Vasilogianni et al., manuscript in preparation).

In summary, this study assessed, for the first time, scaling factors specific for patients with CRLM and showed significantly lower MPPGL in cancerous tissue compared with histologically normal tissue from patients with CRLM. HomPPGL and CPPGL did not differ significantly between cancerous and histologically normal samples. Donor demographics (age, sex, BMI) and the anatomic origin of samples (liver lobe) had no effect on MPPGL and CPPGL values. PBPK simulations on drugs with different extraction ratios metabolized by P450s revealed substantial difference in drug exposure, up to 3.3-fold, when comparing default scaling factors to population-specific scalars. It is therefore recommended that appropriate population-specific MPPGL values, accounting for percentage of liver/tumorous liver tissue, should be considered for prediction of drug exposure in patients with cancer. Future studies should quantify enzyme abundance differences to improve understanding of metabolic drug clearance in cancer.

Acknowledgments

The authors would like to thank the Manchester University National Health Service Foundation Trust (MFT), Biobank, Manchester, UK, for access to liver samples.

Authorship Contributions

Participated in research design: Vasilogianni, Achour, Peters, Barber, Rostami-Hodjegan.

Conducted experiments: Vasilogianni, Achour.

Performed data analysis: Vasilogianni, Achour, Scotcher.

Wrote or contributed to the writing of the manuscript: Vasilogianni, Achour, Scotcher, Peters, Al-Majdoub, Barber, Rostami-Hodjegan.

References

Achour B, Al Feteisi H, Lanucara F, Rostami-Hodjegan A, and Barber J (2017) Global proteomic analysis of human liver microsomes: Rapid characterization and quantification of hepatic drug-metabolizing enzymes. *Drug Metab Dispos* **45**:666–675.

Achour B, Barber J, and Rostami-Hodjegan A (2011) Cytochrome P450 Pig liver pie: determination of individual cytochrome P450 isoform contents in microsomes from two pig livers using liquid chromatography in conjunction with mass spectrometry [corrected]. *Drug Metab Dispos* **39**:2130–2134.

Barter ZE, Bayliss MK, Beaune PH, Boobis AR, Carlile DJ, Edwards RJ, Houston JB, Lake BG, Lipscomb JC, Pelkonen OR, et al. (2007) Scaling factors for the extrapolation of in vivo metabolic drug clearance from in vitro data: reaching a consensus on values of human microsomal protein and hepatocellularity per gram of liver. *Curr Drug Metab* **8**:33–45.

Barter ZE, Chowdry JE, Harlow JR, Snawder JE, Lipscomb JC, and Rostami-Hodjegan A (2008) Covariation of human microsomal protein per gram of liver with age: absence of influence of operator and sample storage may justify interlaboratory data pooling. *Drug Metab Dispos* **36**:2405–2409.

Bates SE, Berry DA, Balasubramaniam S, Bailey S, LoRusso PM, and Rubin EH (2015) Advancing clinical trials to streamline drug development. *Clin Cancer Res* **21**:4527–4535.

Billington S, Ray AS, Salphati L, Xiao G, Chu X, Humphreys WG, Liao M, Lee CA, Mathias A, Hop CECA, et al. (2018) Transporter expression in noncancerous and cancerous liver tissue from donors with hepatocellular carcinoma and chronic hepatitis C infection quantified by LC-MS/MS proteomics. *Drug Metab Dispos* **46**:189–196.

Boogaard PJ, Sumner SC-J, and Bond JA (1996) Glutathione conjugation of 1,2:3,4- diepoxybutane in human liver and rat and mouse liver and lung in vitro. *Toxicol Appl Pharmacol* **136**:307–316.

Bray F, Ferlay J, Soerjomataram I, Siegel RL, Torre LA, and Jemal A (2018) Global cancer statistics 2018: GLOBOCAN estimates of incidence and mortality worldwide for 36 cancers in 185 countries. *CA Cancer J Clin* **68**:394–424.

Cubitt HE, Houston JB, and Galetin A (2011) Prediction of human drug clearance by multiple metabolic pathways: integration of hepatic and intestinal microsomal and cytosolic data. *Drug Metab Dispos* **39**:864–873.

Darwich AS, Ogungbenro K, Hatley OJ, and Rostami-Hodjegan A (2017) Role of pharmacokinetic modeling and simulation in precision dosing of anticancer drugs. *Transl Cancer Res* **6**:S1512–S1529.

Gao J, Zhou J, He XP, Zhang YF, Gao N, Tian X, Fang Y, Wen Q, Jia LJ, Jin H, et al. (2016) Changes in cytochrome P450s-mediated drug clearance in patients with hepatocellular carcinoma in vitro and in vivo: a bottom-up approach. *Oncotarget* **7**:28612–28623.

Guengerich FP, Martin MV, Sohl CD, and Cheng Q (2009) Measurement of cytochrome P450 and NADPH-cytochrome P450 reductase. *Nat Protoc* **4**:1245–1251.

Gutierrez ME, Kummar S, and Giaccone G (2009) Next generation oncology drug development: opportunities and challenges. *Nat Rev Clin Oncol* **6**:259–265.

Hakooz N, Ito K, Rawden H, Gill H, Lemmers L, Boobis AR, Edwards RJ, Carlile DJ, Lake BG, and Houston JB (2006) Determination of a human hepatic microsomal scaling factor for predicting in vivo drug clearance. *Pharm Res* **23**:533–539.

Hemming AW, Reed AI, Howard RJ, Fujita S, Hochwald SN, Caridi JG, Hawkins IF, and Vauthey JN (2003) Preoperative portal vein embolization for extended hepatectomy. *Ann Surg* **237**:686–691, discussion 691–693.

Holch JW, Demmer M, Lamersdorf C, Michl M, Schulz C, von Einem JC, Modest DP, and Heinemann V (2017) Pattern and dynamics of distant metastases in metastatic colorectal cancer. *Visc Med* **33**:70–75.

Houk BE, Bello CL, Kang D, and Amantea M (2009) A population pharmacokinetic meta-analysis of sunitinib malate (SU11248) and its primary metabolite (SU12662) in healthy volunteers and oncology patients. *Clin Cancer Res* **15**:2497–2506.

Hudachek SF, Eckhardt SG, Hicks B, and Gustafson DL (2010) Population pharmacokinetic model of PI-88, a heparanase inhibitor. *Cancer Chemother Pharmacol* **65**:743–753.

Jiang Z, Li C, Zhao Z, Liu Z, Guan X, Yang M, Li X, Yuan D, Qiu S, and Wang X (2018) Abnormal liver function induced by space-occupying lesions is associated with unfavorable oncologic outcome in patients with colorectal cancer liver metastases. *BioMed Res Int* **2018**:9321270.

Lane CS, Nisar S, Griffiths WJ, Fuller BJ, Davidson BR, Hewes J, Welham KJ, and Patterson LH (2004) Identification of cytochrome P450 enzymes in human colorectal metastases and the surrounding liver: a proteomic approach. *Eur J Cancer* **40**:2127–2134.

Li J, Wu J, Bao X, Honea N, Xie Y, Kim S, Sparreboom A, and Sanai N (2017) Quantitative and mechanistic understanding of AZD1775 penetration across human blood-brain barrier in glioblastoma patients using an IVIVE-PBPK modeling approach. *Clin Cancer Res* **23**:7454–7466.

Lipscomb JC, Fisher JW, Confer PD, and Byczkowski JZ (1998) In vitro to in vivo extrapolation for trichloroethylene metabolism in humans. *Toxicol Appl Pharmacol* **152**:376–387.

Lipscomb JC, Teuschler LK, Swartout JC, Striley CAF, and Snawder JE (2003) Variance of microsomal protein and cytochrome P450 2E1 and 3A forms in adult human liver. *Toxicol Mech Methods* **13**:45–51.

Mutch E, Nave R, McCracken N, Zech K, and Williams FM (2007) The role of esterases in the metabolism of ciclesonide to desisobutyryl-ciclesonide in human tissue. *Biochem Pharmacol* **73**:1657–1664.

Pelkonen O, Kaltiala EH, Larmi TKI, and Kärki NT (1973) Comparison of activities of drug-metabolizing enzymes in human fetal and adult livers. *Clin Pharmacol Ther* **14**:840–846.

Pelkonen O, Kaltiala EH, Larmi TKI, and Kärki NT (1974) Cytochrome P-450-linked monooxygenase system and drug-induced spectral interactions in human liver microsomes. *Chem Biol Interact* **9**:205–216.

Piotrovsky VK, Huang ML, Van Peer A, and Langenaecken C (1998) Effects of demographic variables on vorozole pharmacokinetics in healthy volunteers and in breast cancer patients. *Cancer Chemother Pharmacol* **42**:221–228.

Renwick AB, Ball SE, Tredger JM, Price RJ, Walters DG, Kao J, Scatina JA, and Lake BG (2002) Inhibition of zaleplon metabolism by cimetidine in the human liver: in vitro studies with subcellular fractions and precision-cut liver slices. *Xenobiotica* **32**:849–862.

Rostami-Hodjegan A (2012) Physiologically based pharmacokinetics joined with in vitro-in vivo extrapolation of ADME: a marriage under the arch of systems pharmacology. *Clin Pharmacol Ther* **92**:50–61.

Rudeck J, Bert B, Marx-Stoelting P, Schönfelder G, and Vogl S (2018) Liver lobe and strain differences in the activity of murine cytochrome P450 enzymes. Toxicology **404-405**:76–85.

Schmucker DL, Woodhouse KW, Wang RK, Wynne H, James OF, McManus M, and Kremers P (1990) Effects of age and gender on in vitro properties of human liver microsomal monooxygenases. *Clin Pharmacol Ther* **48**:365–374.

Siegel RL, Miller KD, and Jemal A (2018) Cancer statistics, 2018. *CA Cancer J Clin* **68**:7–30.

Suri A, Chapel S, Lu C, and Venkatakrishnan K (2015) Physiologically based and population PK modeling in optimizing drug development: A predict-learn-confirm analysis. *Clin Pharmacol Ther* **98**:336–344.

Wilson ZE, Rostami-Hodjegan A, Burn JL, Tooley A, Boyle J, Ellis SW, and Tucker GT (2003) Inter-individual variability in levels of human microsomal protein and hepatocellularity per gram of liver. *Br J Clin Pharmacol* **56**:433–440.

Wong VKH, Malik HZ, Hamady ZZR, Al-Mukhtar A, Gomez D, Prasad KR, Toogood GJ, and Lodge JPA (2007) C-reactive protein as a predictor of prognosis following curative resection for colorectal liver metastases. *Br J Cancer* **96**:222–225.

Yoshida K, Budha N, and Jin JY (2017) Impact of physiologically based pharmacokinetic models on regulatory reviews and product labels: Frequent utilization in the field of oncology. *Clin Pharmacol Ther* **101**:597–602.

Zhang H, Gao N, Tian X, Liu T, Fang Y, Zhou J, Wen Q, Xu B, Qi B, Gao J, et al. (2015) Content and activity of human liver microsomal protein and prediction of individual hepatic clearance in vivo. *Sci Rep* **5**:17671.

Address correspondence to: Amin Rostami-Hodjegan, Centre for Applied Pharmacokinetic Research, School of Health Sciences, The University of Manchester, Stopford Building, Oxford Road, Manchester, M13 9PT, UK; E-mail address: amin.rostami@manchester.ac.uk